JOURNAL OF GUIDANCE, CONTROL, AND DYNAMICS
Vol. 24, No. 2, March–April 2001

Agility Metric Robustness Using Linear Error Theory

David Smith* and John Valasek†
Texas A&M University, College Station, Texas 77843-3141

The robustness of agility metrics has been studied to determine the sensitivity of selected metrics to variations in initial conditions and uncertainties in physical characteristics and coefficients. The selected metrics are time to roll through bank angle metric, time-averaged integral of pitch rate metric, and power onset/loss parameter. Each metric was evaluated with initial condition errors and parametric uncertainties of physical constants using linear error theory to validate the use of linear approximations to propagate the errors.

Nomenclature

b	=	wingspan, ft
C_L	=	lift coefficient
C_{l_p}	=	change in rolling moment due to roll rate; also roll damping derivative
$C_{l_{\delta a}}$	=	change in rolling moment due to aileron deflection
D	=	drag, lbs
g	=	gravitational constant, ft/s^2
I_{xx}	=	body x-axis moment of inertia, slug-ft^2
n_z	=	load factor, g
P_s	=	specific excess power, ft/s
$\bar{q}$	=	dynamic pressure, lbs/ft^2
S	=	wing area, ft^2
T	=	thrust, lbs
V	=	velocity, ft/s
W	=	aircraft weight, lbs
δa	=	aileron deflection, deg
ρ	=	density, slug/ft^3
ϕ	=	bank angle, deg
$\dot{\psi}$	=	turn rate, deg/s

Introduction

FIGHTER agility metrics, or, simply, agility metrics, are measures of merit intended to quantify and compare the combat effectiveness of fighter type aircraft.[1,2] They differ from traditional steady-state measures such as maximum speed, maximum load factor, and maximum sustained turn rate in that they describe the transient capability of the aircraft, or how the aircraft transitions from one steady-state flight condition to another. This consideration is an important one since technology improvements in engines, thrust vectoring, and all-aspect missiles have decreased the time of engagements and increased the transient aspect of maneuvering.

Numerous metrics have been proposed to quantify agility, and many of them have been collected and analyzed in Ref. 1. Although some researchers have focused on defining agility by either postulating metrics from a largely empirical approach[3,4] or from a strictly mathematical sense,[5,6] still others have taken the existing metrics and used them to compare the capability of different aircraft,[1] and to understand how to design flight control systems for agility.[7,8] In an effort to standardize agility flight testing, a standard evaluation maneuver set was developed,[9] and agility metrics have been flight tested under the Agile Lighting and Agile Thunder projects at the United States Air Force Test Pilot School.[10]

An important aspect not directly addressed in the preceding works reviewed is the robustness of agility metrics to deviations in pilot inputs, aircraft model errors/uncertainties, and initial condition errors. Robustness is especially relevant for application to autonomous Unmanned Combat Aerial Vehicles (UCAV) where the measurement of agility online, in real-time, is needed to help shape optimal trajectories that are being determined on-the-fly for a variety of combat tasks.[11] Valasek and Downing[1] investigated the effects of deviations in pilot inputs on several agility metrics using standardized inputs applied to four different batch-type aircraft simulations. The results confirmed that precise, repeatable pilot inputs (preferably from an automated source) are desirable to generate accurate agility metric data. More important, allowable upper bounds of deviations in pilot inputs were quantified. Many agility metrics are not simply the measurement of a single state but either a differential equation or an algebraic equation that is a function of measurements. These equations can be parameterized, and the sensitivity of aircraft maneuvers to structured parametric uncertainties was investigated in Ref. 12. Six parameters of the aircraft model (weight, thrust, drag, maximum lift coefficient, maximum roll rate, and roll mode time constant) were varied assuming a uniform distribution and evaluated using nine different maneuvers. The nine maneuvers studied included level accelerations, three level turns at different Mach numbers and load factors, split-S, flat scissors, rolling scissors, defensive spiral, and turn initiation. Results indicated large sensitivity to uncertainty in aircraft weight and lower sensitivity to uncertainties in thrust, drag, and maximum lift coefficient. Uncertainties in roll parameters were found to be unimportant except for turn initiation.

How measurement errors propagate with time through the differential or algebraic agility equations is still an open research area. The question to be answered is, which particular equations are robust with respect to errors and by how much? Errors cannot be avoided altogether, but if errors can be shown to propagate linearly with time through an equation, then agility results obtained with that equation may be considered acceptable. However, if it can be shown that errors propagate nonlinearly with time through the equation, then agility results obtained with those equations can realistically be regarded with skepticism or discarded altogether.

This paper develops a framework for analyzing the sensitivity of agility metrics to initial condition and structured parametric uncertainties without the need to resort to time-consuming and costly Monte Carlo analysis. Linear error theory is used to quantify the robustness of a selected set of agility metrics, and the results are then verified with both time histories and traditional Monte Carlo methods.

Linear Error Theory

Linear error theory is a method of error propagation and of measuring the validity of linearity assumptions for nonlinear dynamic systems. This method applies to both algebraic and nonlinear dynamic systems. First, consider the algebraic model of the form

$$\boldsymbol{y} = A\boldsymbol{x} + b \tag{1}$$

where $\boldsymbol{y} \in \mathbb{R}^{m \times 1}$ and $\boldsymbol{x} \in \mathbb{R}^{n \times 1}$ are random vectors, and $b \in \mathbb{R}^{m \times 1}$ and $A \in \mathbb{R}^{m \times n}$ are known constant matrices. The expected values, or means, of $\boldsymbol{x}$ and $\boldsymbol{y}$ are

$$\bar{\boldsymbol{x}} = E\{\boldsymbol{x}\} \tag{2}$$

$$\bar{\boldsymbol{y}} = E\{\boldsymbol{y}\} \tag{3}$$

Received 18 October 1999; accepted for publication 21 April 2000.

*Graduate Research Assistant, Department of Aerospace Engineering. Student Member AIAA.

†Assistant Professor, Department of Aerospace Engineering. Senior Member AIAA.

where $E\{\cdot\}$ is the expectation operator defined as

$$E\{\boldsymbol{x}\} = \int \boldsymbol{x} g(\boldsymbol{x})\, dx \tag{4}$$

Here, $\boldsymbol{x}$ is any arbitrary value of $\boldsymbol{x}$ and $g(\boldsymbol{x})$ is the probability density function of $\boldsymbol{x}$. Substituting Eq. (1) into Eq. (3) yields

$$\bar{\boldsymbol{y}} = A\bar{\boldsymbol{x}} + b \tag{5}$$

The covariance matrices of $\boldsymbol{x}$ and $\boldsymbol{y}$ are defined as

$$P_{xx} = E\{(\boldsymbol{x} - \bar{\boldsymbol{x}})(\boldsymbol{x} - \bar{\boldsymbol{x}})^T\} \tag{6}$$

$$P_{yy} = E\{(\boldsymbol{y} - \bar{\boldsymbol{y}})(\boldsymbol{y} - \bar{\boldsymbol{y}})^T\} \tag{7}$$

Furthermore, the difference between $\boldsymbol{y}$ and the expected value of $\boldsymbol{y}$ can be related to the difference between $\boldsymbol{x}$ and the expected value of $\boldsymbol{x}$ by the equation

$$(\boldsymbol{y} - \bar{\boldsymbol{y}}) = A(\boldsymbol{x} - \bar{\boldsymbol{x}}) \tag{8}$$

By substituting Eq. (8) into Eq. (7), the covariance of $\boldsymbol{y}$ is related to the covariance of $\boldsymbol{x}$ by the similarity transformation

$$P_{yy} = A P_{xx} A^T \tag{9}$$

The second system is the nonlinear, nonautonomous, dynamic system

$$\dot{\boldsymbol{x}} = f(t, \boldsymbol{x}), \qquad \boldsymbol{x}(t_0) = \boldsymbol{x}_0 \tag{10}$$

where $\boldsymbol{x}(t)$ denotes the state vector at time t. Small departures from a reference trajectory $\bar{\boldsymbol{x}}(t)$ can be denoted by

$$\delta\boldsymbol{x}(t) = \boldsymbol{x}(t) - \bar{\boldsymbol{x}}(t) \tag{11}$$

Linearization of Eq. (10) about the reference trajectory $\bar{\boldsymbol{x}}(t)$ results in the following linear differential equation

$$\delta\dot{\boldsymbol{x}} = J\delta\boldsymbol{x} \tag{12}$$

where

$$J = \left[\frac{\partial f}{\partial \boldsymbol{x}}\right]_{\bar{x}} \tag{13}$$

such that

$$\delta\boldsymbol{x}(t) = \Phi(t, t_0)\delta\boldsymbol{x}(t_0) \tag{14}$$

Here, the Jacobian matrix J is obtained by taking the partial differentiation of Eq. (1) evaluated about the reference trajectory. The expression $\Phi(t, t_0)$ in Eq. (14) is the state transition matrix from initial time to current time t and satisfies

$$\dot{\Phi}(t, t_0) = J\Phi(t, t_0) \tag{15}$$

subject to

$$\Phi(t, t_0) = I \tag{16}$$

Initial condition uncertainty in Eq. (10) can be represented as the additive Gaussian errors $\delta\boldsymbol{x}(t_0)$ with known covariance matrix $P(t_0)$, defined as

$$P(t_0) = E\left\{\delta\boldsymbol{x}(t_0) \quad \delta\boldsymbol{x}(t_0)^T\right\} \tag{17}$$

where $E\{\cdot\}$ is the expectation operator defined as

$$E\{f(\boldsymbol{x})\} = \int f(\boldsymbol{x}) g(\boldsymbol{x})\, d\boldsymbol{x} \tag{18}$$

In Eq. (17), $f(\boldsymbol{x})$ is any arbitrary function of the state variable $\boldsymbol{x}$ and $g(\boldsymbol{x})$ is the probability density function. The propagation of the error covariance matrix along the nonlinear trajectory can be computed by using the similarity transformation

$$P(t) = \Phi(t, t_0) P(t_0) \Phi^T(t, t_0) \tag{19}$$

The severity of the nonlinearity can be measured by the use of a nonlinearity index, which is the error in the transition matrix normalized by the transition matrix of the reference tranjectory. Since linearity has been assumed, the Jacobian would be constant. Using this, Junkins defines the dynamic nonlinearity index in Ref. 13 as

$$\upsilon(t, t_0) \equiv \sup_i \frac{\|\Phi_i(t, t_0) - \Phi(t, t_0)\|_2}{\|\Phi(t, t_0)\|_2} \tag{20}$$

Here, the $\sup(\cdot)$ operator extracts the maximum value of $(\cdot)$ over the range of points sampled at time t on the trajectory $\boldsymbol{x}_i(t)$, and the $\|(\cdot)\|_2$ denotes the Frobenious norm of a matrix. The value of υ can range from zero (linear) to one (very nonlinear). The uncertainties can be assumed to propagate linearly if $\upsilon < 10^{-2}$. If this value restriction holds, standard linear approximations and methods can be used. If the nonlinearity index is larger than this value, then the linear approximations are not valid, and other nonlinear methods must be used.

Analysis Procedure

The procedure used by the authors to evaluate each agility metric is presented here. If Gaussian distributed errors produce Gaussian distributed outputs, then the errors propagating linearly. The purpose of the Monte Carlo analysis is to verify the linear error theory analysis by applying this test to the Monte Carlo results. The step-by-step procedure is as follows:

1) Parameterize agility metric.

2) Identify parameters for initial condition errors and for parametric uncertainties.

3) Calculate Jacobians of parameterized metric with respect to the identified parameters from step 2.

4) Calculate the nonlinearity index for initial condition errors and parametric uncertainties for metric errors.

5) Verify the results with Monte Carlo analysis.

Selected Agility Metrics

Agility metrics are categorized by the type of aircraft motion and the amount of time the maneuver requires. Aircraft maneuvers are broken down by the three axes: longitudinal metrics, lateral metrics, and axial metrics. Metrics are also described either as transient (small time scales of about 2–3 s) or as functionals, which usually require 10–30 s to complete. Three agility metrics were studied in this investigation. A transient time-scale metric from each axis was selected. The three metrics are shown in Table 1.

Each metric was parameterized in terms of the aircraft state variables, physical constants and coefficients, control inputs, and time. What follows is a description of each metric, the parameterized form of the metric, and a description of each term.

Lateral: Time to Roll Through Bank Angle

The definition of the lateral metric is the time required to roll through a target bank angle at various angles of attack.[10] The parameterized equation for bank angle as a function of time for a step input is given in Eq. (21):

$$\Delta\phi = \frac{8C_{l_{\delta a}}\delta_a I_{xx}}{\rho S b^3 C_{l_p}^2}\left[\exp\left(\frac{V\rho S b^2 C_{l_p} t}{4I_{xx}}\right) - \frac{V\rho S b^2 C_{l_p} t}{4I_{xx}} - 1\right] \tag{21}$$

Table 1 Classifying the selected metrics

Axis	Transient metric
Longitudinal	Time averaged integral of pitch rate
Lateral	Time to roll through bank angle
Axial	Power onset/loss parameter

The lateral metric was selected because it was easily parameterized and because the metric is a good measure of the transient performance aspect of the aircraft's lateral agility.

Longitudinal: Time-Averaged Integral of Pitch Rate

The longitudinal metric is defined as the average pitch rate over the time interval $t_2 - t_1$, where t_1 is the time at which the pitch maneuver is executed and t_2 is selected at the discretion of the tester.[1] The parameterized equation for average pitch rate is given in Eq. (22):

$$\text{avg } q = \frac{\int_{t_1}^{t_2} q \, \mathrm{d}t}{t_2 - t_1} \tag{22}$$

The longitudinal metric was selected because it quantifies the sustainable pitch rate of the aircraft instead of just the maximum value obtained at an instant in time. Thus, this metric relates to the task-oriented ability of the aircraft to point the nose or to achieve a desired load factor.

Axial: Power Onset/Loss Parameter

The power onset/loss parameter is defined as the increment of specific excess power resulting in going from a minimum/maximum energy condition to a maximum/minimum energy condition divided by the time required to complete the transition.[4] The parameterized metric is shown in Eq. (23):

$$\dot{P}_s = \frac{\mathrm{d}}{\mathrm{d}t}\left[\frac{V(T - D)}{W}\right] \tag{23}$$

The power onset/loss parameter quantifies the effects of maximum thrust, drag of the aircraft, and engine spool time. The acceleration of the aircraft is included in the time derivative of velocity. The maximum thrust of the engine is included in the thrust term, and the engine spool effect is included in the time derivative of thrust term. The drag characteristics of the aircraft are encompassed in both the drag and the time derivative of drag terms.

Initial Condition Error Results

Each selected agility metric was studied for sensitivity to initial condition errors and parametric uncertainties. The initial condition errors were changes in velocity, thrust, and drag; the parametric uncertainties were introduced as changes in physical properties and coefficients in the parameterized equations. The analysis was performed using the technique derived from linear error theory. The metric was first evaluated at a nominal condition for altitude, velocity, and maneuver sequence. Then the metric was evaluated with the initial condition and parametric variations. The amount of variation for each parameter was based on the research of Hoffren and Vilenius,[12] Roskam,[14] and studies performed by the authors. Most of the variations were 10% changes in value. The analysis was performed using the UCAV 6 nonlinear, non-real-time, flight simulation computer program. The UCAV 6 simulation is a six-degree-of-freedom simulation with steady nonlinear aerodynamics up to a 90-deg angle of attack. This simulation is an unmanned version of an AV-8B Harrier simulation.

The physical characteristics of the UCAV 6 model are listed in Table 2.

Table 2 UCAV 6 model physical characteristics

Characteristic	Value
Gross weight	13,350 lb
Wing area	533 ft^2
Wing span	46.2 ft
Mean geometric chord	11.53 ft
I_{xx}	16,425 slug-ft^2
I_{yy}	26,000 slug-ft^2
I_{zz}	54,284 slug-ft^2
I_{xz}	0

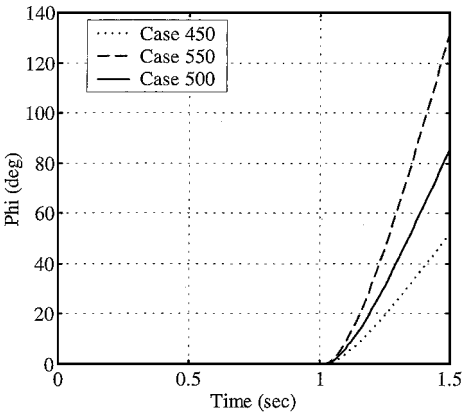

Fig. 1 Bank angle response time history.

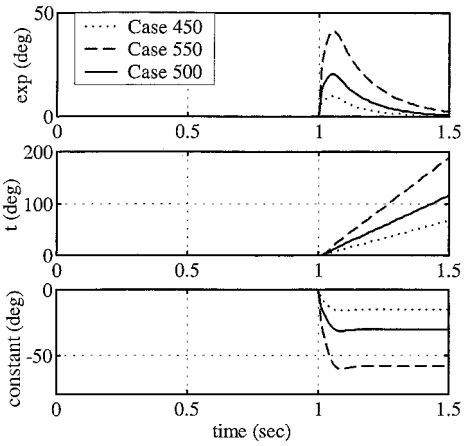

Fig. 2 Roll metric component time histories.

Time to Roll Through Bank Angle

The nominal initial state of the test was at an altitude of a 1000 ft, a velocity of 500 fps, and an aileron input command of 27 deg at time equals 1.0 s. The nominal case was designated Case 500. The initial condition error variation was a change in velocity of ±50 fps. Additionally, parametric variations were a ΔC_{l_p} of ±15%, a $\Delta C_{l_{\delta a}}$ of ±25%, and a ΔI_{xx} of ±10%. Case 450 was the combination of the −50 fps velocity error, the −25% error in $C_{l_{\delta a}}$, the −10% error in I_{xx}, and the 15% variation in C_{l_p}, and Case 550 was the opposite combination of variations. Figure 1 shows the bank angle response for this metric.

Results show Case 450 increased the time to roll through a target bank angle. For Case 550, the time to roll through a target bank angle decreased. Also indicated here is that the performance robustness of the roll metric is fairly good, as there is only a 0.1-s difference at a target bank angle of 45 deg.

Roll metric results can be broken up into the components of Eq. (21), an exponential term, a linear term with respect to time, and a constant term. The time history of these three components is shown in Fig. 2. The exponential term rises quickly after the input is commanded, and then decays rapidly. The linear term is the dominant component, as this component is the largest in magnitude for the maneuver. The constant component is shown in the bottom plot of the figure.

The nonlinearity index was calculated for these results and is shown in Fig. 3. The index rises sharply after 1 s due to the commanded aileron deflection, and then slowly increases as the linear component of Eq. (21) for the off-nominal test cases diverges from the nominal case.

Results show that the metric is strongly nonlinear during the command input, and increases slightly afterward. The roll metric is strongly nonlinear to initial condition errors, as the nonlinearity index is more than an order of magnitude larger than the acceptable value.

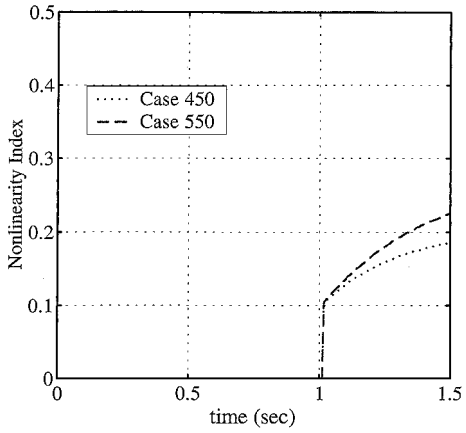

Fig. 3 Nonlinearity index time history for the roll metric.

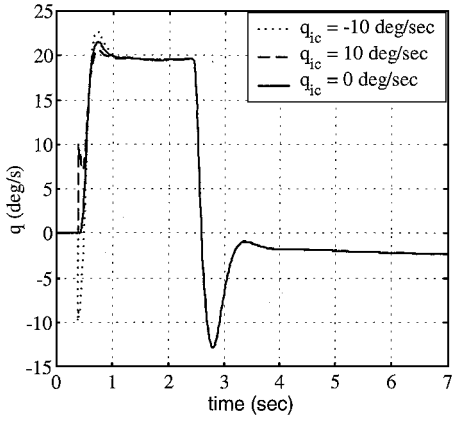

Fig. 4 Pitch rate response time history.

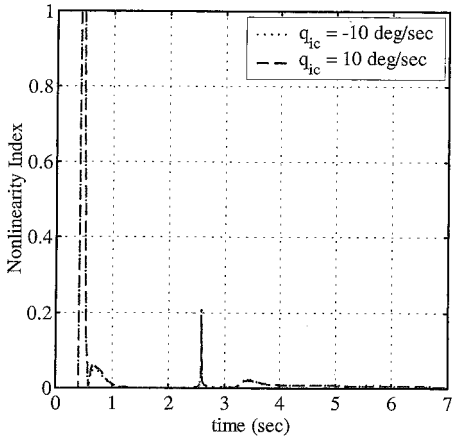

Fig. 5 Nonlinearity index time history for average pitch rate metric.

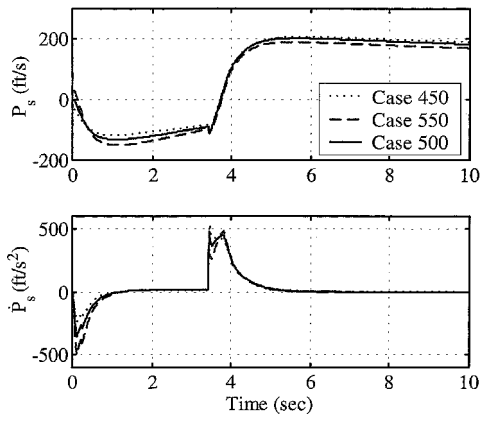

Fig. 6 Specific excess power and power onset parameter time histories.

Time-Averaged Integral of Pitch Rate

The time-averaged integral of pitch rate metric was studied using a nominal initial state of a 1000-ft altitude and a velocity of 500 fps. The input command for the study was maximum aft stick at time equals 0.5 s, hold for 2 s, and then forward stick to unload the aircraft to zero load factor at time equals 2.5 s. The initial condition error variation was an initial pitch rate error of ± 10 deg/s at time equals 0.38 s.

The pitch rate response is shown in Fig. 4. The nominal time-averaged integral of pitch rate was 3.896 deg/s, the positive pitch rate error case result was 4.011 deg/s, and the negative pitch rate error case result was 3.839 deg/s. These initial condition errors result

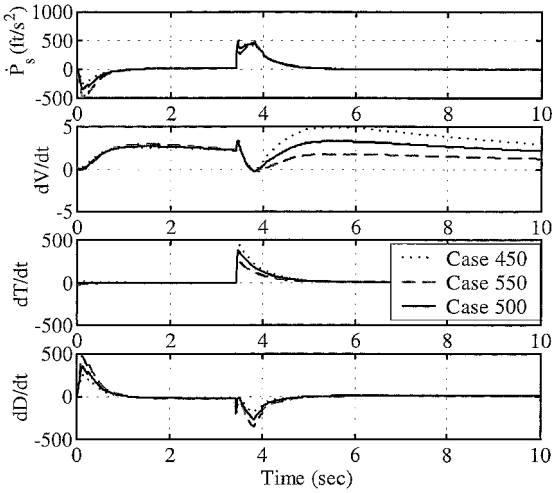

Fig. 7 Power onset parameter component time histories.

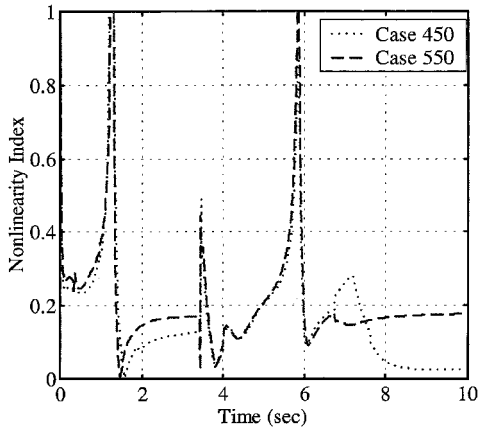

Fig. 8 Nonlinearity index time history for power onset parameter metric.

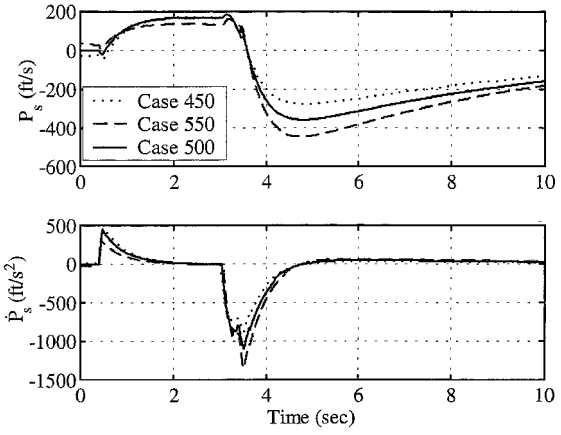

Fig. 9 Specific excess power and power loss parameter time histories.

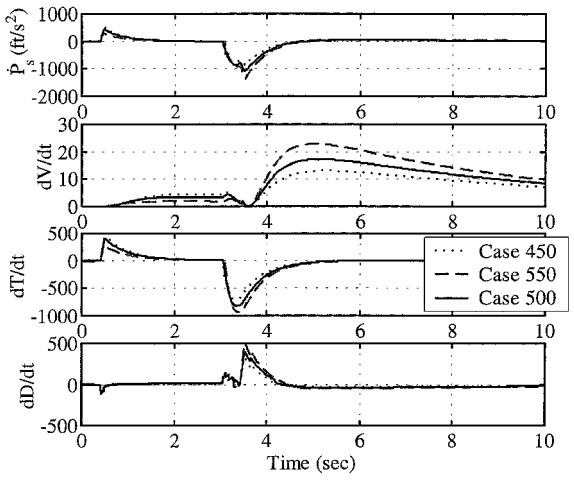

Fig. 10 Power loss parameter component time histories.

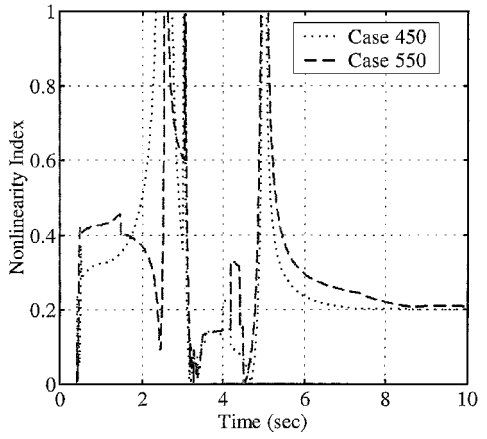

Fig. 11 Nonlinearity index time history for power loss parameter metric.

in only a small change in pitch rate and in average pitch rate. This indicates that the performance robustness of the average pitch rate metric is very good.

The average pitch rate metric is fairly linear with respect to initial condition error in pitch rate. This relationship is shown in the nonlinearity index result vs time of Fig. 5. The sharp rises after 0.5 and 2.5 s are the result of the longitudinal stick commands. The width of the first peak is also due to the pitch rate error introduced in the off-nominal cases. The small rise after 3.5 s coincides with the pitch rate steadying out near zero. Afterward, the index decreases when the pitch rate is nearly constant and the average pitch rate decreases slowly.

Power Onset Parameter

The power onset parameter metric was studied using a nominal initial state of a 1000-ft altitude and a velocity of 500 fps. Initially, the speed brake was deployed at time equals 0.1 s and is retracted at time equals 3.5 s. Full throttle was commanded at time equals 3.5 s. The nominal test was designated Case 500. The initial condition error variations were a change in velocity of ± 50 fps, a change in thrust of a $\pm 10\%$, and a change in drag of $\pm 10\%$. Two off-nominal cases were tested. For Case 450, the -50-fps velocity error was grouped with the -10% thrust error and the 10% drag error; Case 550 was the combination of the 50-fps velocity error, the 10% thrust error, and the -10% drag error.

The time history of specific excess power P_s and the power onset parameter are shown in Fig. 6. The maximum error in P_s is only about 20 fps, and the maximum power onset parameter error is about 150 ft/s^2 right after the speed brake and again at the throttle inputs. Otherwise, the error for the power onset parameter was around 5 ft/s^2. The power onset parameter value for the nominal case was 138.598 ft/s^2. For Case 450, the power onset parameter value was 127.655 ft/s^2, and for Case 550, the power onset parameter was equal to 139.467 ft/s^2. As a result, the performance robustness of the power onset parameter metric indicates a variation specific excess power and power onset parameter due to initial condition errors.

As was discussed in the Selected Metric section, the power onset parameter is composed of three components: 1) a time derivative

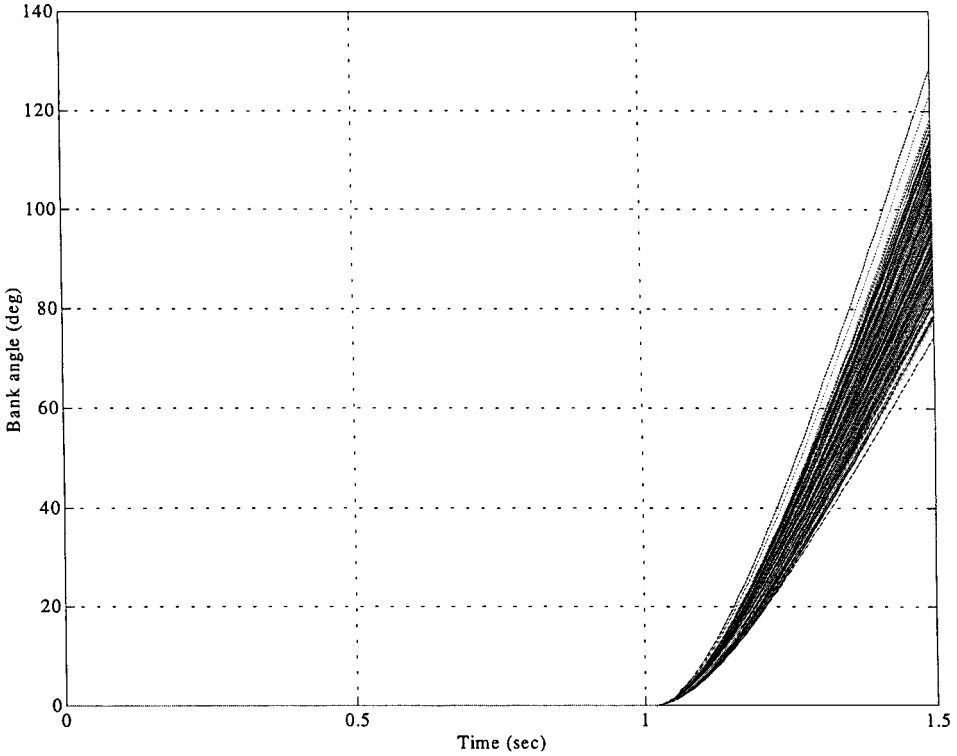

Fig. 12 Time histories of bank angle: Monte Carlo results.

of velocity term times the difference of thrust and drag divided by the aircraft weight, 2) a time derivative of thrust times velocity term divided by the aircraft weight, and 3) a time derivative of drag term times velocity divided by the aircraft weight.

This expanded version of Eq. (23) is shown here:

$$\dot{P}_s = \frac{\mathrm{d}V}{\mathrm{d}t}\left[\frac{(T-D)}{W}\right] + \frac{\mathrm{d}T}{\mathrm{d}t}\left(\frac{V}{W}\right) + \frac{\mathrm{d}D}{\mathrm{d}t}\left(\frac{V}{W}\right) \qquad (24)$$

Each of these components is plotted respectively in Fig. 7. Both nominal and off-nominal cases exhibit the following trends. The first component influences only a small amount, as the maximum magnitude is less than 5 ft/s^2 for the acceleration component, and the time derivative of drag component is large for only a few tenths of a second. The time derivative of thrust term and time derivative of drag term are the primary components of the power onset parameter, as the maximum magnitude of the thrust-dot and drag-dot terms are almost 500 ft/s^2 before slowly decaying.

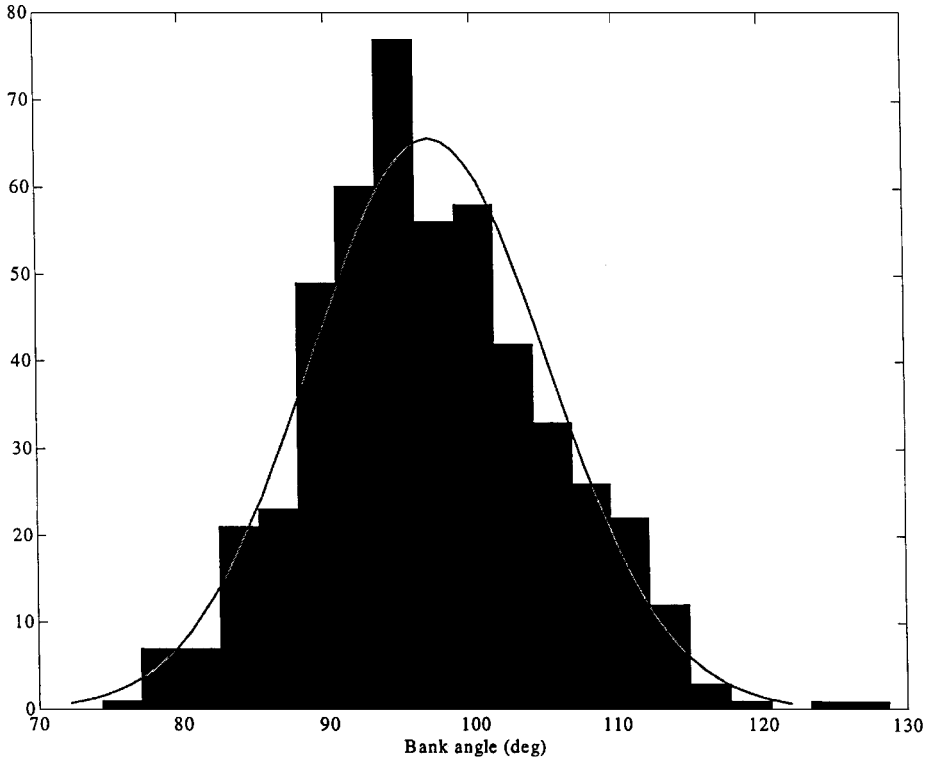

Fig. 13 Distribution of bank angle: Monte Carlo results.

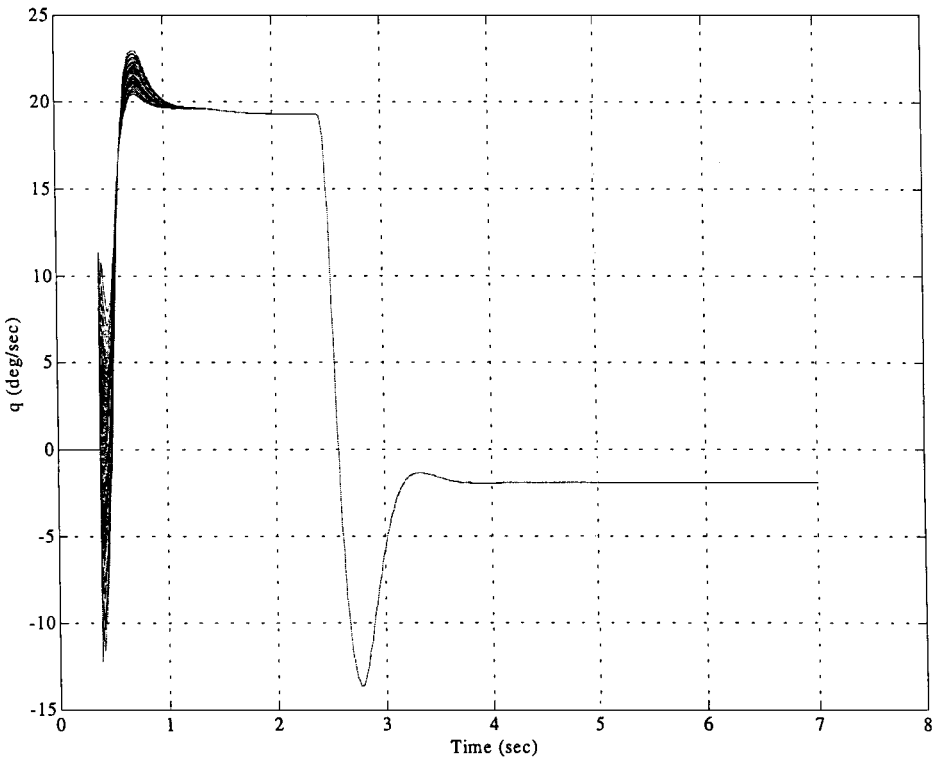

Fig. 14 Time histories of pitch rate response: Monte Carlo results.

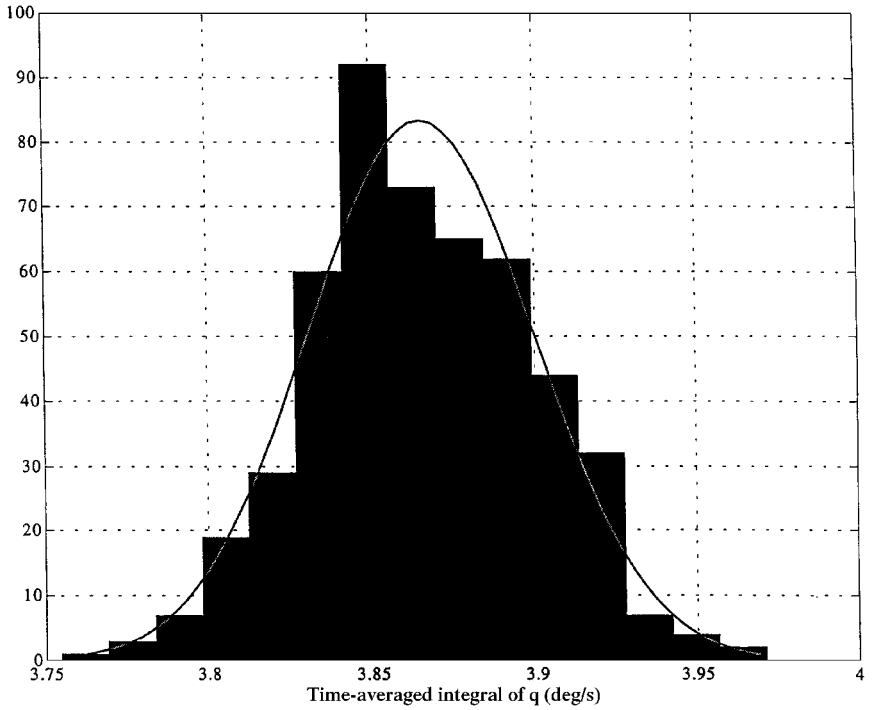

Fig. 15 Distribution of time-averaged integral of pitch rate: Monte Carlo results.

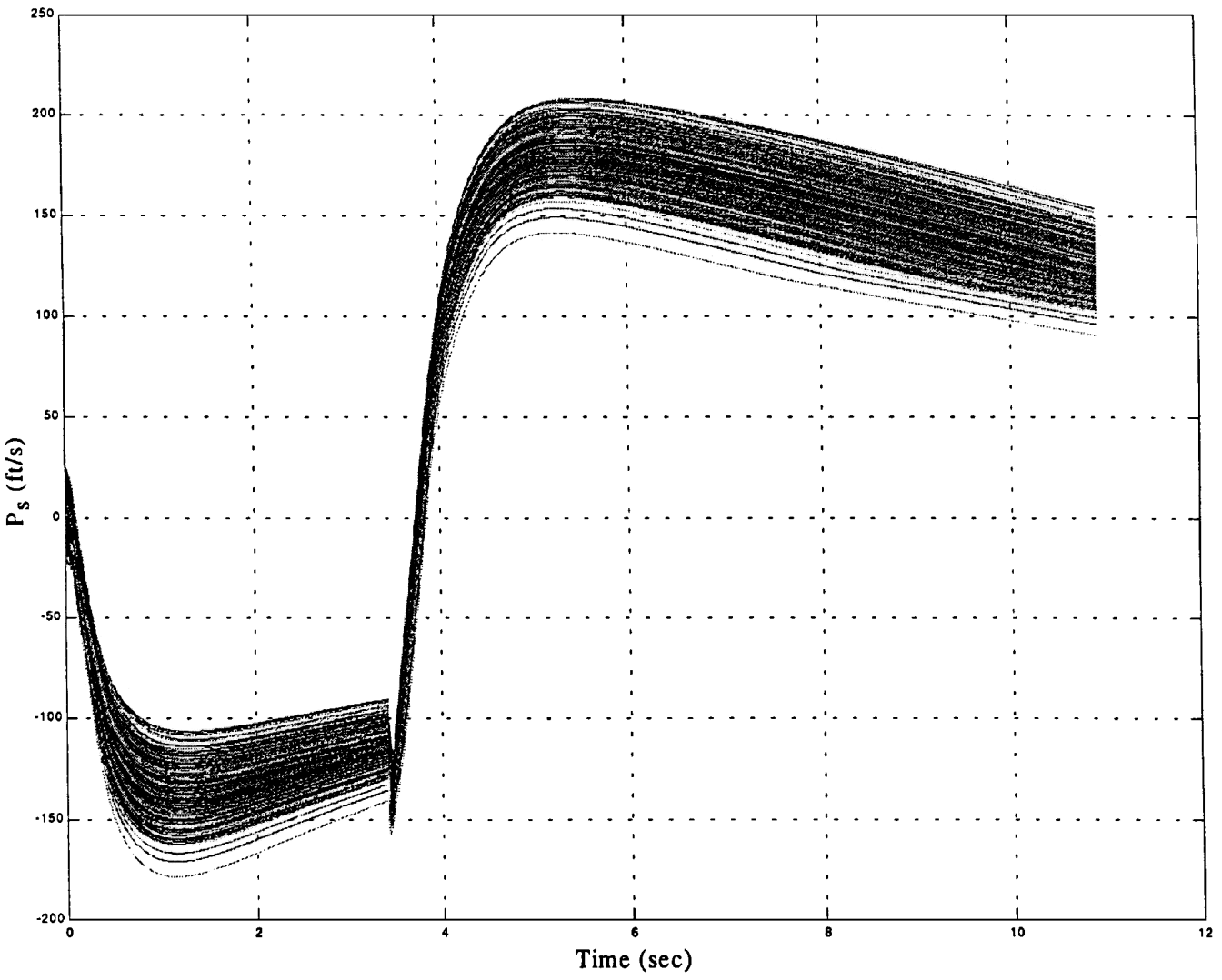

Fig. 16 Time histories of specific excess power: Monte Carlo results.

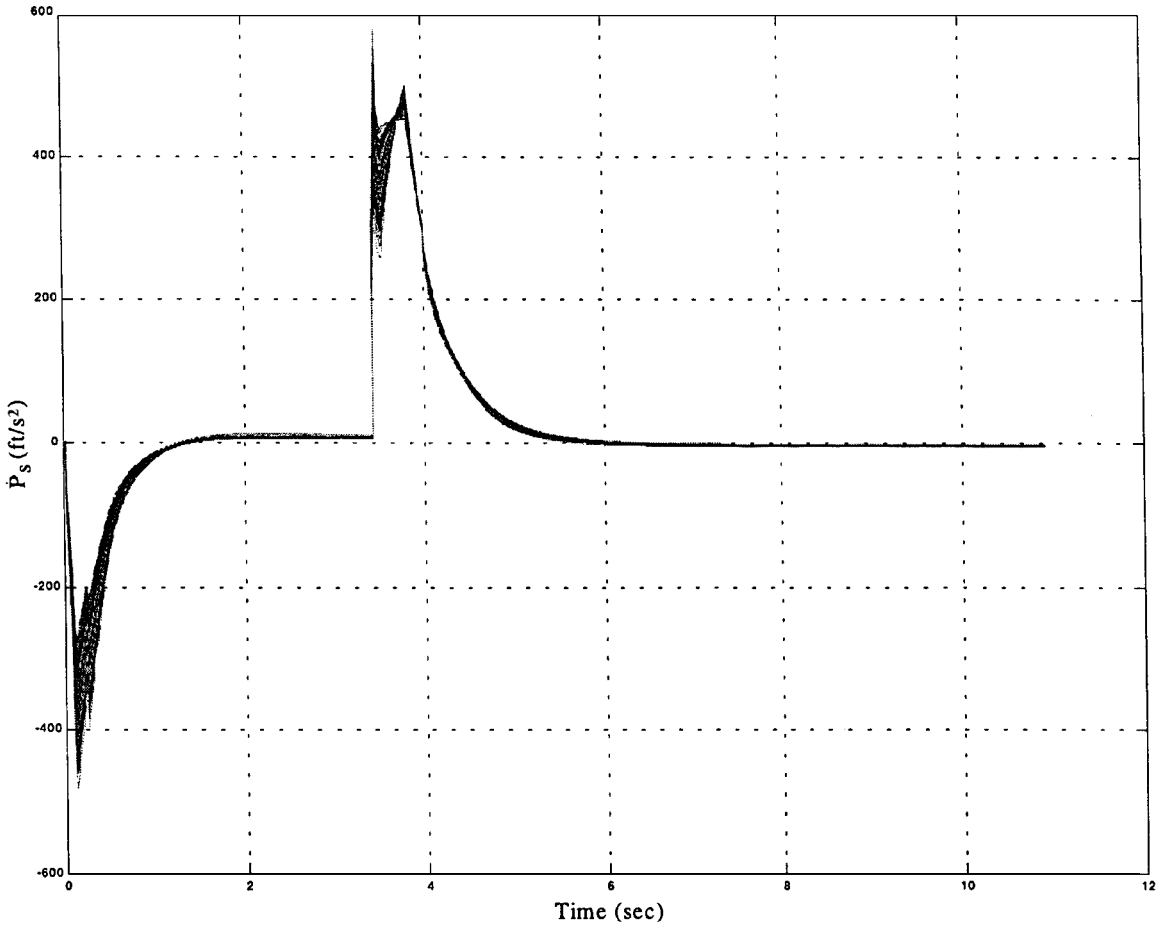

Fig. 17 Time histories of power onset parameter: Monte Carlo results.

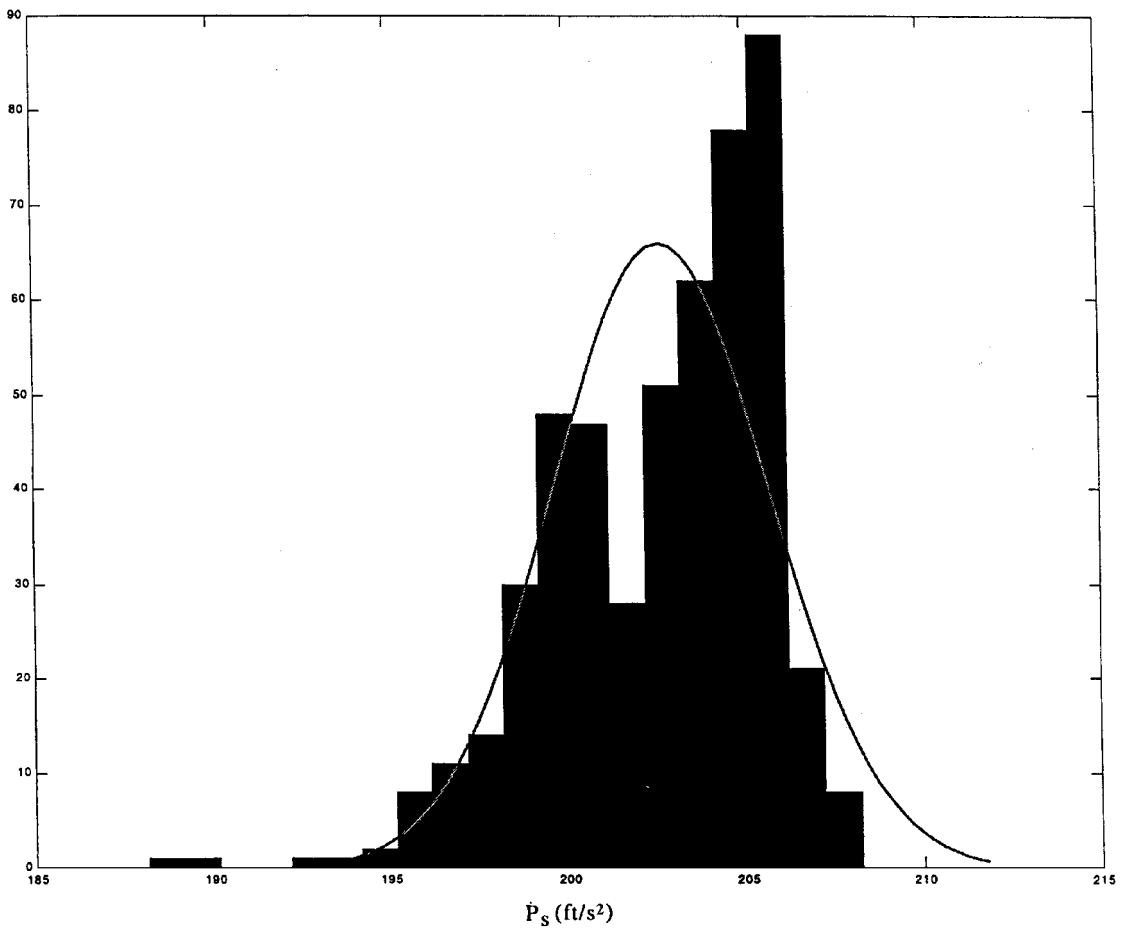

Fig. 18 Distribution of power onset parameter: Monte Carlo results.

The nonlinearity index for the power onset parameter is plotted in Fig. 8 for the two off-nominal test cases. Initially, the metric is strongly nonlinear as the initial condition errors are introduced, and then the nonlinearity index decreases rapidly. The large spike around time equals 1.0 s is due to the drag reaching a maximum due to the speed-brake input. The combination of the speed brake being retracted and the throttle input at time equals 3.5 s causes the next sharp spike in the index. As the thrust increases, the nonlinearity index grows from 4 to 6 s, where thrust reaches a maximum value. Results of the power onset parameter show that the nonlinearity index is strongly nonlinear to initial condition errors, especially near times of throttle and speed-brake inputs. After the inputs are commanded, the nonlinearity index remains relatively constant.

Power Loss Parameter

The power loss parameter metric was studied using a nominal initial state of 1000-ft altitude and a velocity of 500 fps. Initially, the throttle was increased 10% at time equals 0.5 s and was then decreased 80% at time equals 3.5 s. The speed brake was deployed at time equals 3.5 s. The nominal test was designated Case 500. The initial condition error variations were a change in velocity of ± 50 fps, a change in thrust of $\pm 10\%$, and a change in drag of $\pm 10\%$. Two off-nominal cases were tested. For Case 450, the -50-fps velocity error was grouped with the -10% thrust error and the 10% drag error; Case 550 was the combination of the 50-fps velocity error, the 10% thrust error, and the -10% drag error.

The specific excess power P_s and power loss parameter are shown vs time in Fig. 9. The maximum error in P_s is about 100 ft/s, and the maximum power loss parameter error is about 250 ft/s^2 right after the speed brake extends and again at the throttle inputs. Otherwise, the error for the power loss parameter was around 20 ft/s^2. The power loss parameter value for the nominal case was -354.408 ft/s^2. For Case 450, the power loss parameter value was -283.338 ft/s^2, and for Case 550, the power loss parameter was equal to -437.189 ft/s^2. As a result, the performance robustness of the power loss parameter metric indicates a variation in specific excess power due to initial condition errors.

Each of the components of the power loss parameter is plotted respectively in Fig. 10. Both nominal and off-nominal cases exhibit the following trends. The first component influences only a small amount, as the maximum magnitude is less than 25 ft/s^2 for the acceleration component. The time derivative of thrust term and time derivative of drag term are the primary components of the power loss parameter, as the maximum magnitude of the thrust-dot component is almost 1000 ft/s^2, and the drag-dot term is almost 500 ft/s^2 before slowly decaying.

The nonlinearity index for the power loss parameter is plotted in Fig. 11 for the two off-nominal test cases. The large spike around time equals 0.5 s is due to the throttle input, and then the increase from around 2 to 3 s is due to the thrust increasing to a maximum. The large spike after 3 s is due to the throttle and speed-brake inputs, and then the large spike after 4 s is due to the drag reaching a maximum due to the speed-brake input. Results of the power loss parameter show that the nonlinearity index is strongly nonlinear due to initial condition errors, especially near times of throttle and speed-brake inputs. After the inputs are commanded, the nonlinearity index remains relatively constant.

Monte Carlo Results

A Monte Carlo analysis was performed for each agility metric with the initial condition errors and parametric uncertainties specified using Gaussian distributions. The mean and variance of each distribution were determined to fit the given range of values for each parameter. The time histories and distribution of results were then compared to the linear error theory results to verify those results. The chi-square goodness of fit was used to get 90% confidence bounds for the distribution of results.

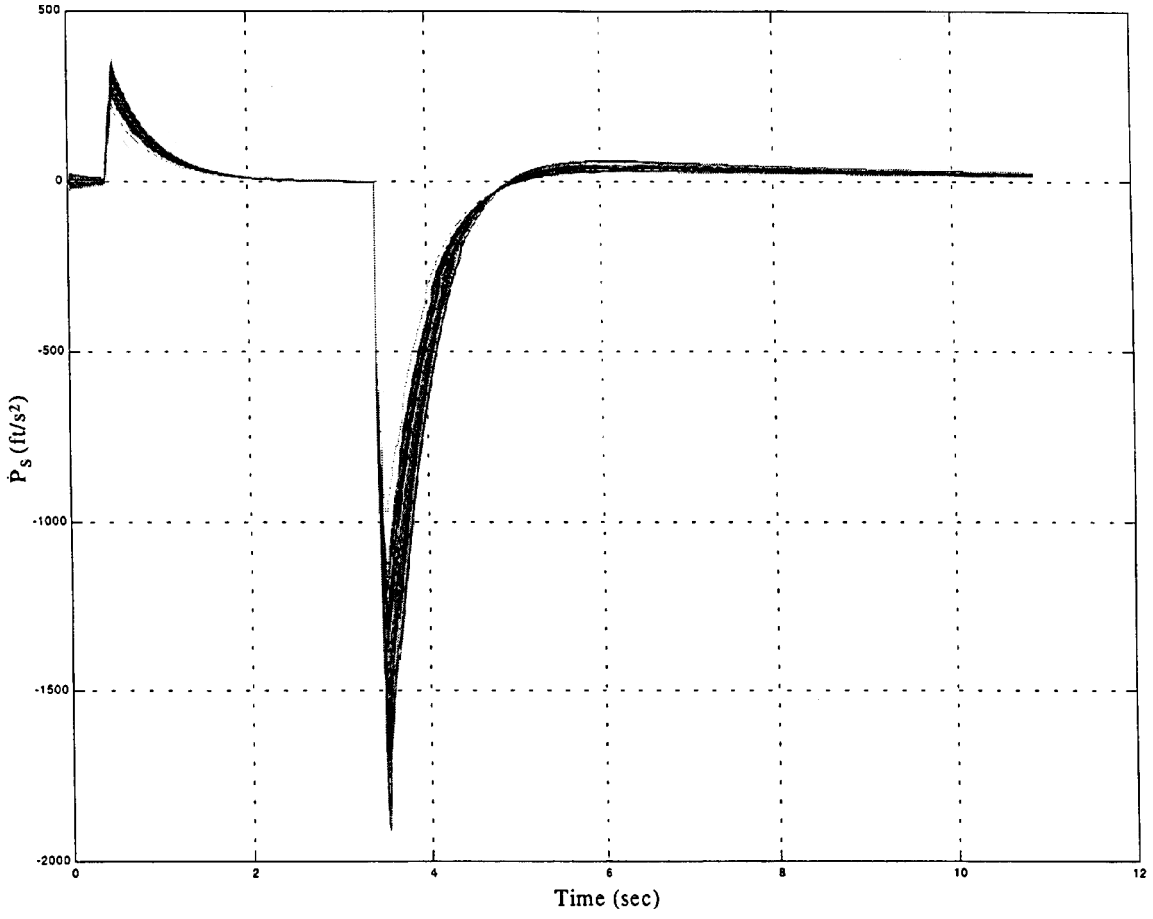

Fig. 19 Time histories of specific excess power: Monte Carlo results.

Time to Roll Through Bank Angle

The bank angle metric was tested using 500 Monte Carlo runs at a nominal initial state of a 1000-ft altitude, a velocity of 500 fps, and an aileron input command of 27 deg at time equals 1.0 s. The variations were Gaussian distributions in velocity with a range of ± 50 fps, in C_{l_p} with a range of $\pm 15\%$, in $C_{l_{\delta_a}}$ with a range of $\pm 25\%$, and in I_{xx} with a range of $\pm 10\%$. Figure 12 shows the bank angle response for these tests. For ease of analysis, the runs lasted for 1.5 s, and the bank angles achieved were compared. Results showed a nearly Gaussian distribution of bank angle with a range of ± 25 deg, as plotted in a histogram in Fig. 13. Also plotted in Fig. 13 is the 90% confidence for a Gaussian distribution with the same mean and variance as the data. The distribution for the bank angle is not a good Gaussian fit.

The Monte Carlo analysis verified the linear error theory analysis. Gaussian distributed input errors did not produce Gaussian distributed outputs. Furthermore, the value of the nonlinearity index for both off-nominal cases was about 0.4; this metric is weakly nonlinear to initial condition errors and parametric uncertainties. This relationship corresponds to the slightly non-Gaussian distribution of the bank angle results.

Time-Averaged Integral of Pitch Rate

The time-averaged integral of pitch rate metric was tested using 500 Monte Carlo runs at the same initial conditions and input command as the linear error theory analysis cases. The initial condition error variation was a Gaussian distribution of initial pitch rate error with a range of ± 10 deg/s at time equals 0.38 s. Figure 14 shows the pitch rate response of the aircraft, and the histogram of the time-averaged integral of pitch rate results is plotted in Fig. 15 with the 90% confidence for a Gaussian distribution with the same mean and variance as the data. The distribution of average pitch rate exhibits a Gaussian distribution and is confirmed by the Monte Carlo analysis. Gaussian distributed input errors did produce Gaussian distributed outputs for the time averaged integral of pitch rate metric.

Power Onset Parameter

The power onset parameter was analyzed using 500 Monte Carlo runs at the same initial conditions and input commands as in the linear error theory analysis section. The initial condition errors were Gaussian distributions of thrust with a range of $\pm 10\%$, of drag with a range of $\pm 10\%$, and of velocity with a range of ± 50 fps. Time histories of specific excess power and power onset parameter are shown in Figs. 16 and 17, respectively. The histogram of the power onset parameter results is shown in Fig. 18 with the 90% confidence Gaussian distribution curve with the same mean and variance as the data. Clearly the distribution is non-Gaussian. This concurs with the nonlinearity index for the power onset parameter, as the distribution indicated the power onset parameter is nonlinear to initial condition errors.

Power Loss Parameter

The power loss parameter was analyzed using 500 Monte Carlo runs at the same initial conditions and input commands as in the linear error theory analysis section. The initial condition errors were Gaussian distributions of thrust with a range of $\pm 10\%$, of drag with a range of $\pm 10\%$, and of velocity with a range of ± 50 fps. Time histories of specific excess power and power loss parameter are shown in Figs. 19 and 20, respectively. The histogram of the power loss parameter results is shown in Fig. 21 with the 90% confidence Gaussian distribution curve with the same mean and variance as the data. The distributed results do not fit the Gaussian curve very

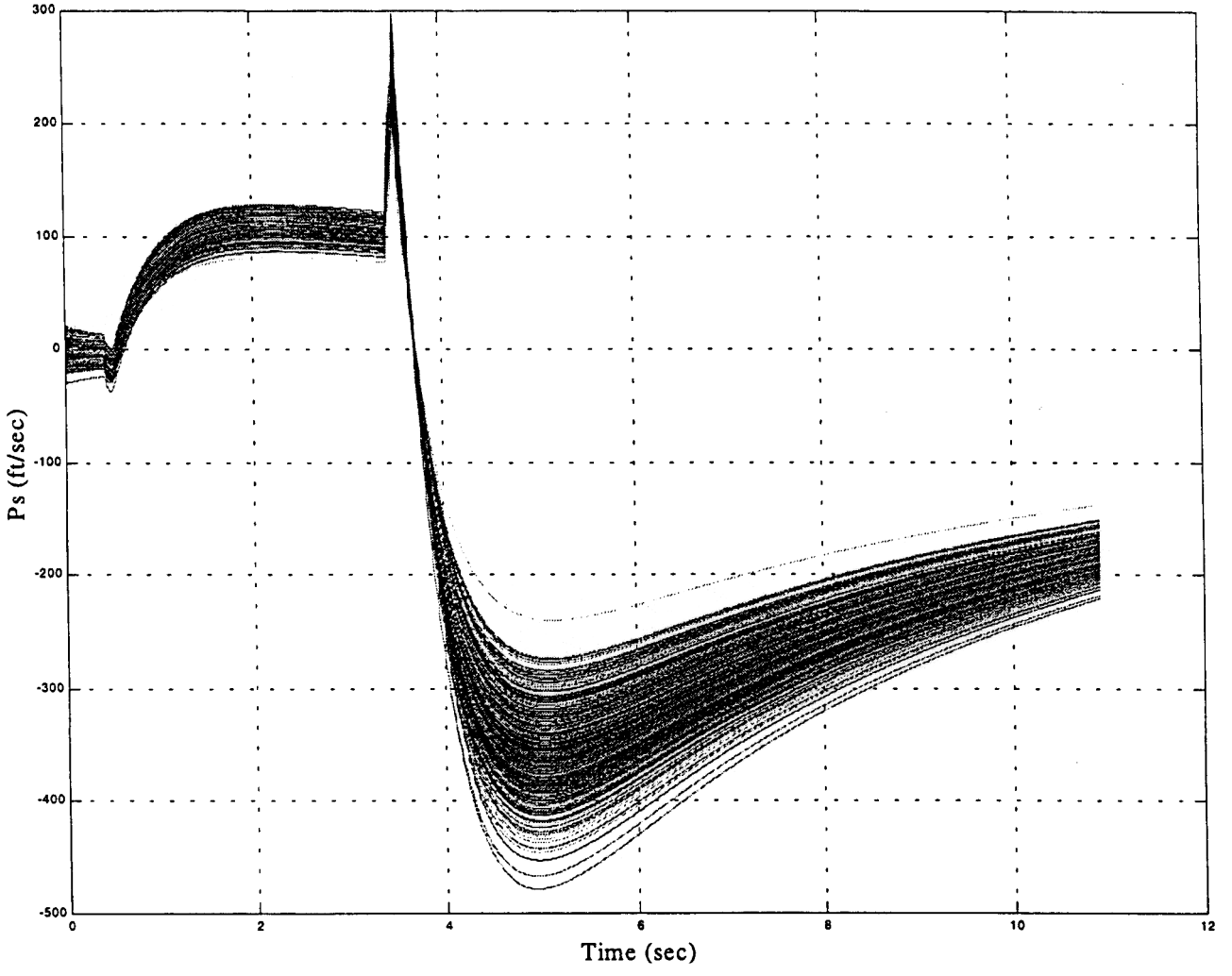

Fig. 20 Time histories of power-loss parameter: Monte Carlo results.

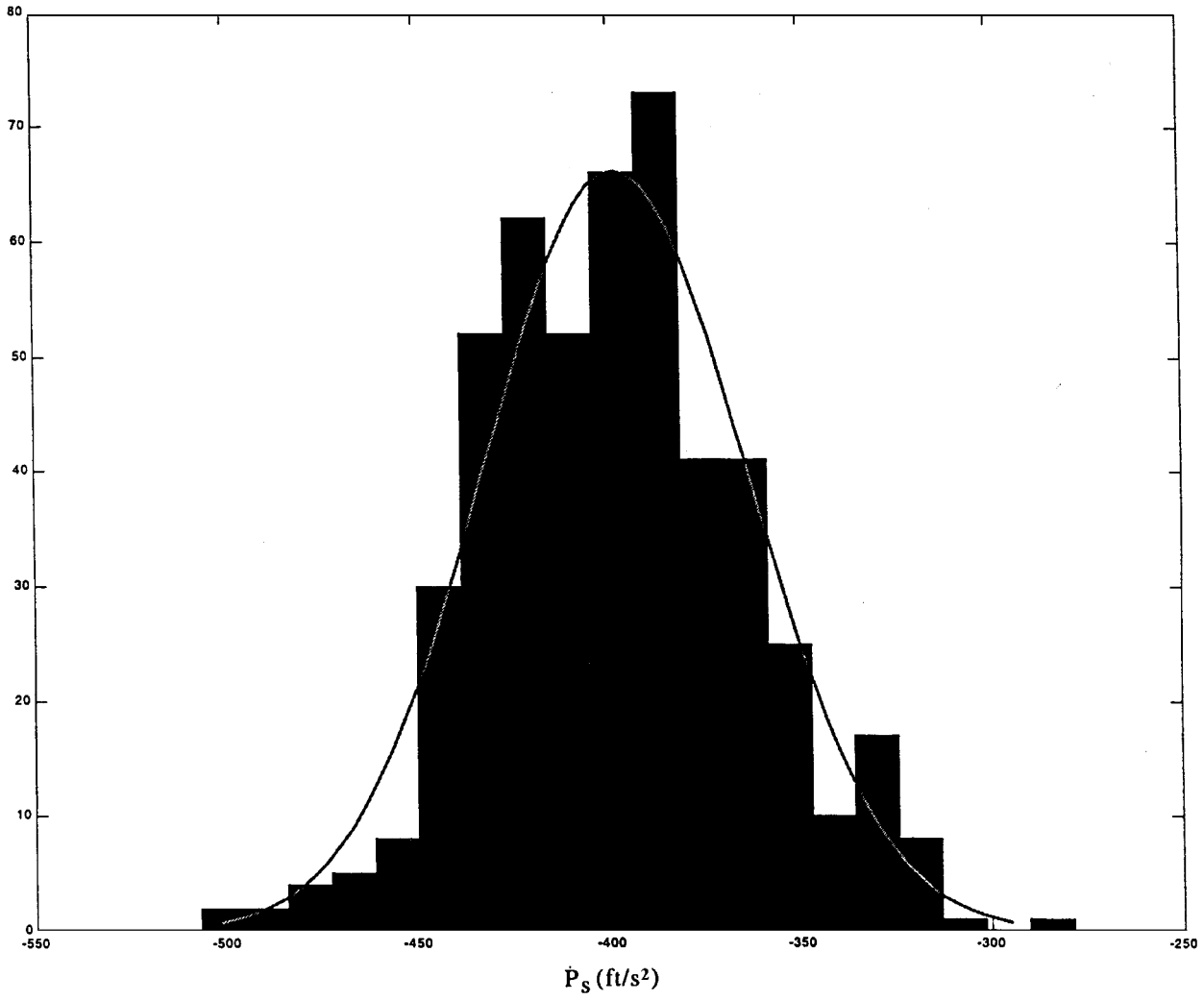

Fig. 21 Distribution of power loss parameter: Monte Carlo results.

well. This concurs with the nonlinearity index for the power loss parameter, as it indicated the power loss parameter is nonlinear to initial condition errors.

Conclusions

The robustness of three agility metrics was evaluated by performing a sensitivity analysis to variations in initial conditions and uncertainties in physical characteristics and stability and control derivatives. Linear error theory was employed to evaluate the use of linear approximations to propagate the initial condition errors forward in time. Based upon the results, several conclusions can be drawn:

1) The time to roll through bank angle metric is largely insensitive to initial condition variations in velocity and parametric uncertainties. However, the roll metric is weakly nonlinear to initial condition errors and parametric uncertainties, and linear methods should not be used to propagate the errors forward in time. Monte Carlo results confirm that the metric is nonlinear to these initial condition and parametric uncertainty variations.

2) The average pitch rate metric is largely insensitive to the initial pitch rate error but is strongly linear with respect to initial condition errors. Thus, linear approximations can be used with confidence to propagate forward the errors. Monte Carlo results confirm that the pitch rate metric is linear to initial condition errors in pitch rate.

3) The power onset parameter metric is insensitive to initial condition errors in velocity, thrust, and drag. However, the metric is strongly nonlinear to initial condition errors, especially during the throttle and speed brake transients where the thrust rate and drag rate terms cause the metric to be strongly nonlinear. The distribution of power onset parameter values from the Monte Carlo analysis confirms that the metric is nonlinear.

4) The performance robustness of the power loss parameter metric showed a dispersion in results compared to the power onset parameter, and thus the metric is sensitive to initial condition errors in velocity, thrust, and drag. The metric is strongly nonlinear to initial condition errors, especially during the throttle and speed brake transients, where the thrust rate and drag rate terms cause the metric to be strongly nonlinear. The distribution of power loss parameter values from the Monte Carlo analysis confirms that the metric is nonlinear.

In summary, a framework for analyzing the sensitivity of agility metrics to initial condition and structured parametric uncertainties using linear error theory has been demonstrated. Future research will focus on correlating the Monte Carlo results with the nonlinearity index results.

Acknowledgments

This research is supported by the United States Navy, Office of Naval Research under Grant N00014-97-1-0938. The monitor is Allen Moshfegh. The authors gratefully acknowledge this support.

References

[1]Valasek, J., Downing, D. R., "An Investigation of Fighter Aircraft Agility," NASA-CR-1954608, Nov. 1993.

[2]Liefer, R. K., Valasek, J., Eggold, D. P., and Downing, D. R., "Fighter Agility Metrics, Research and Test," *Journal of Aircraft*, Vol. 29, No. 3, 1992, pp. 452–457.

[3]Kalviste, J., "Measures of Merit for Dynamic Aircraft Maneuvering," Society of Automotive Engineers, Paper 901005, April 1990.

[4]Skow, A., Hodgkinson, J., Ettinger, R., Parker, R., and Foltyn, R., "Transient Agility Enhancements for Tactical Aircraft, Volume II," Eidetics International, TR 89-001, Torrance, CA, Jan. 1989.

[5]Mazza, C. J., "Agility: A Rational Development of Fundamental Metrics and Their Relationships to Flying Qualities," *AGARD Conference Proceedings 508: Flying Qualities*, AGARD, Oct. 1990, pp. 342–348.

[6]Herbst, W. B., "Future Fighter Maneuverability for Air Combat," *Proceedings of the AIAA Design, Systems, and Operations Meeting*, Oct. 1993, pp. 151–156.

[7]Eggold, D. P., Valasek, J., and Downing, D. R., "Measurement and Improvement of the Lateral Agility of the F-18," *Journal of Aircraft*, Vol. 30, No. 6, 1993, pp. 803, 804.

[8]Murphy, P. C., and Davidson, J. B., "A Control Law Design Method Facilitating Control Power, Robustness, Agility, and Flying Qualities Tradeoffs: CRAFT," NASA/TP-1998-208463, Sept. 1998, p. 45.

[9]Klyde, D. H., and Mitchell, D. G., "Handling Quality Demonstration Maneuvers for Fixed Wing Aircraft. Volume II: Maneuver Catalog," Flight Dynamics Directorate, Wright Lab., Air Force Material Command, WL-TR-97-3100, Wright–Patterson AFB, OH, Oct. 1997.

[10]Brown, P., Hardeman, J. W., Ross, M. L., Albrecht, B. R., Fortman, K. M., and Zeis, J. E., Jr., "T-38A/F-16B Agility Metrics Evaluation (Agile Lightning)," U.S. Air Force Test Pilot School TR USAFTPS-TR-87A-SO4, Dec. 1987.

[11]Krishnamurthy, K., and Ward, D., "An Intelligent Inference Engine for Autonomous Aerial Vehicles," AIAA Paper 99-4251, Aug. 1999.

[12]Hoffren, J., and Vilenius, J., "Sensitivity of Air Combat Maneuvers to Aircraft-Modeling Uncertainties," AIAA Paper 98-4165, Aug. 1998.

[13]Junkins, J. L., "Adventures on the Interface of Dynamics and Control," *Journal of Guidance, Control, and Dynamics*, Vol. 20, No. 6, 1997, pp. 1060–1063.

[14]Roskam, J., *Airplane Flight Dynamics and Automatic Flight Controls, Part 1*, Roskam Aviation and Engineering Corp., Ottawa, KS, 1979, p. 236.